JACS
JOURNAL OF THE AMERICAN CHEMICAL SOCIETY

ARTICLE

pubs.acs.org/JACS

Supramolecular Hybrid of Gold Nanoparticles and Semiconducting Single-Walled Carbon Nanotubes Wrapped by a Porphyrin−Fluorene Copolymer

Hiroaki Ozawa,[†] Xun Yi,[‡] Tsuyohiko Fujigaya,[†] Yasuro Niidome,[†] Tanemasa Asano,[‡] and Naotoshi Nakashima*[,†,§,∥]

[†]Department of Applied Chemistry, Graduate School of Engineering, [‡]Department of Electronics, Graduate School of Information Science and Electrical Engineering, and [∥]WPI-I[2]CNER, Kyushu University, Motooka744, Nishi-ku, Fukuoka 819-0395, Japan

[§]Core Research of Evolutional Science & Technology (CREST), Japan Science and Technology Agency, 5 Sanbancho, Chiyoda-ku, Tokyo 102-0075, Japan

Supporting Information

ABSTRACT: We describe the design, synthesis, and characterization of a supramolecular hybrid of gold nanometals and semiconducting single-walled carbon nanotubes (SWNTs) wrapped by a porphyrin−fluorene copolymer (**1**), as well as fabrication of a thin-film transistor (TFT) device using the hybrid. Photoluminescence mapping revealed that the copolymer selectively dissolved SWNTs with chirality indices of (8,6), (8,7), (9,7), (7,6), and (7,5); dissolution of (8,6), and (8,7) SWNTs was especially efficient. The solubilized SWNTs were connected to gold nanoparticles (AuNPs) via a coordination bond to prepare a supramolecular hybrid composed of AuNPs/copolymer **1**-wrapped SWNTs, which were studied by atomic force and scanning and transmission electron microscopies. A fabricated TFT device using the semiconducting SWNTs/copolymer **1** shows evident p-type transport with an On/Off ratio of ∼10^5. The transport properties of the TFT changed after coordination of the AuNPs with the SWNTs/copolymer **1**.

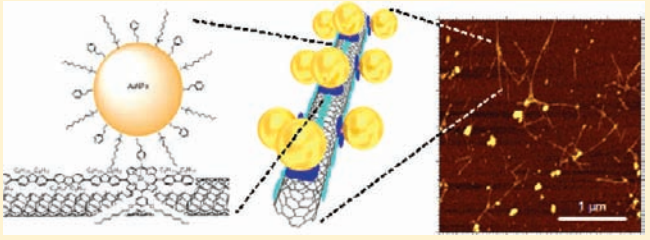

INTRODUCTION

Carbon nanotubes (CNTs) have attracted great interest in both fundamental science and applications over a wide area due to their unique and remarkable electronic, optical, mechanical, and thermal properties.[1−16] Recently, many attempts to design, prepare, and analyze composites and hybrids of CNTs and metal nanoparticles (MNPs) have been reported, based on methods using covalent and/or noncovalent functionalization,[17−19] especially thiol-functionalized CNTs with MNPs[20−24] because of their potential application in nanoelectronic devices, sensing, catalysts, etc. The CNTs used in such studies are extensively oxidized by strong acid treatments to form COOH-functionalized CNTs, which are used to introduce a thiol moiety. However, COOH-functionalized CNTs lose intrinsic CNT properties due to damage on the π-conjugated CNT structure.

Several reports describing the preparation of CNT/MNP composites using noncovalent-functionalized CNTs have been published.[20−24] Ellis et al. reported the connection of octanethiol-capped gold nanoparticles (AuNPs) to CNTs by hydrophobic interactions.[25] Mono- and polycyclic aromatic ring-terminated alkylamines were used by Ou et al. as the linkers to fabricate CNT/MNPs.[26] Assembly of AuNPs onto DNA-wrapped SWNTs and solution-phase synthesis of SWNT/MNP assemblies that can be generally applied to common metal elements have been reported.[27,28] Microwave irradiation combined with the polyol method was reported to form monodispersed AuNPs uniformly on the CNT surfaces.[29] Nanoparticles or nanocrystals have been directly functionalized on CNT surfaces by chemical reactions.[30] However, for these studies, the coexistence of metallic and semiconducting SWNTs with many chiralities creates an obstacle to both fundamental studies and practical applications.[31] Thus, it is important to develop a method for preparing CNT/MNP hybrids using SWNTs having a specified chirality.

Herein, we report a novel strategy for preparing a supramolecular hybrid fabricated from only semiconducting SWNTs and AuNPs. For this purpose, we designed and synthesized copolymer **1** (Figure 1), consisting of fluorene and Zn(II)-porphyrin backbones. Chirality-selective recognition/extraction of the SWNTs is one of the central issues in nanotube science.[32] Polyfluorene (PFO) and PFO derivatives are known to selectively solubilize semiconducting SWNTs in toluene.[33,34] The Zn(II)-porphyrin moiety on copolymer **1** is an anchor for introducing MNPs via coordination bonding. After formation of a film of copolymer **1**/semiconducting SWNTs, a solution of pyridine-terminated AuNPs was placed on the film to prepare a AuNPs/copolymer **1**/SWNT

Received: June 16, 2011
Published: August 10, 2011

dx.doi.org/10.1021/ja2055885 | J. Am. Chem. Soc. 2011, 133, 14771–14777

hybrid material via coordination of the pyridinyl moiety to the zinc(II) of the porphyrin units (Figure 2), which was characterized by atomic force microscopy (AFM), scanning electron microscopy (SEM), and transmission electron microscopy (TEM). We also describe the fabrication of a thin-film transistor (TFT) using the SWNTs/copolymer **1** hybrid and report our finding that the transport properties changed after coordination of the AuNPs with copolymer **1** in the hybrid.

EXPERIMENTAL SECTION

Instruments. ^{1}H NMR spectra were recorded using a Bruker AV300M spectrometer. Analytical gel permeation chromatography (GPC) data were recorded using a MD-2015 Plus instrument (JASCO) with TSK-GEL α-3000 and TSK-GEL α-M gels (TOSO). THF was used as the mobile phase at a flow rate of 0.5 mL/min. UV−vis−NIR absorption and photoluminescence (PL) spectra were recorded on V-570 (JASCO) and FluorologR-3 (Horiba-Jobin Yvon) spectrophotometers, respectively. Raman spectra (excitation at 633 and 514 nm) were recorded using LabRAM ARAMIS (Horiba) and RM1000B (Ranishaw) spectrometers. AFM images of the samples were recorded using a NanoScope III (Veeco) instrument. SEM and TEM images were measured using JSM-6700F and JEM-2010 microscopes (JEOL), respectively. X-ray photoelectron spectroscopy (XPS) was carried out using a 5800 ESCA (PHI) spectrophotometer. Measurements of fabricated device properties were recorded using a HP 4156C semiconducting analysis machine (Agilent) with a probe station.

Materials. As-produced SWNTs (HiPco; the length and diameter of the pristine SWNTs are 1−10 μm and 0.8−1.2 nm, respectively) were purchased from Unidym, Inc. and were used as received.

Copolymer 1. Copolymer **1** was synthesized via Yamamoto coupling reaction:[35] $Ni(COD)_2$ (100 mg, 0.36 mmol), 2,2′-dipyridyl (57 mg, 0.36 mmol), 1,5-cyclooctadiene (0.1 mL), dried DMF (0.5 mL), and dried toluene (1.0 mL) were placed in a flask and heated at 80 °C for 30 min under a nitrogen flow to obtain a dark purple complex. 2,7-Dibromo-9,9′-dioctylfluorene (60 mg, 0.11 mmol) and 5,15-dibromo-10,20-[3,5-bis(octyloxyphenyl)]porphyrinatozinc (12 mg, 0.01 mmol) were dissolved in dried toluene (1.0 mL), and the mixture was added to the dark purple solution. The subsequent mixture was maintained at 80 °C for 48 h and then poured into methanol (50 mL) and filtered. The obtained solid was dissolved in dichloromethane and passed through a filter to remove the residue. After removal of dichloromethane under reduced pressure, the concentrated solution was added to methanol (50 mL) to give a precipitate, which was filtered and dried under vacuum at room temperature to provide copolymer **1** as a dark red-orange solid (42 mg). ^{1}H NMR ($CDCl_3$, 300 MHz): δ 9.31−8.8 (m, β-position), 8.34−7.94 (m, Ph), 7.94−7.68 (m, fluorene), 6.9−6.75 (m, Ph), 4.06 (m, OCH_2), 2.11 (m, CH_2), 1.84 (m, CH_2), 1.1−1.5 (m, CH_2), 0.85−0.80 (m, CH_3). UV−vis (toluene): λ_{max} = 384, 426 nm. Fluorescence (toluene, λ_{ex} = 382 nm), λ_{em} = 413, 440, 530 nm.

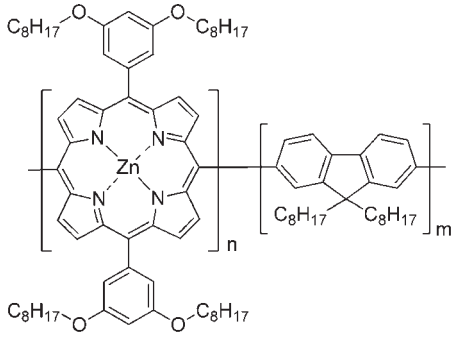

copolymer **1** (n=1, m=10), copolymer **2** (n=1, m=2)

Figure 1. Chemical structure of copolymers **1** and **2**. The composition ratios of the porphyrin unit (n) to the fluorene unit (m) are 1:10 and 1:2, respectively.

Copolymer **2** was synthesized and characterized in a similar manner. ^{1}H NMR ($CDCl_3$, 300 MHz): δ 9.31−8.8 (m, β-position), 8.34−7.94 (m, Ph), 7.94−7.68 (m, fluorene), 6.9−6.75 (m, Ph), 4.06 (m, OCH_2), 2.11 (m, CH_2), 1.84 (m, CH_2), 1.1−1.5 (m, CH_2), 0.85−0.80 (m, CH_3).

Preparation of Py-AuNPs/Copolymer 1/SWNT Hybrid. Pyridine-coated gold nanoparticles (py-AuNPs) were synthesized according to the literature.[36] 4-Pyridineethanethiol (10 mg, 0.72 mmol) was added to a *tert*-dodecanethiol-coated AuNP (*t*-dode-AuNPs; 10 mg) solution in toluene (10 mL) with stirring for 1 day. The obtained reaction solution was centrifuged at 2000*g* for 30 min, and the supernatant was removed. The residue was dissolved in MeOH and centrifuged (2000*g*, 30 min) again to give a precipitate which was removed, and then the solvent was evaporated. The obtained solid was washed with toluene three times and then dried to give the product as a black powder (7.0 mg).

The SWNTs (1.0 mg) were added to copolymer **1** (1.0 mg) dissolved in toluene (6.0 mL) and sonicated with a bath-type ultrasonic cleaner (Branson 2210) for 1 h, followed by centrifugation at 10000*g* for 1 h (Hitachi Himac CS 100GL instrument). The top 80% of the supernatant was passed through a filter (Advantec, Inc., PTFE; pore size 100 nm), and the obtained solid was washed with toluene; additional toluene (6 mL) was added, and the mixture was resonicated for 30 min, followed by centrifugation at 150000*g* for 1 h. A 100 μL portion of the obtained copolymer **1**/SWNT solution was placed on silicon or a fresh mica substrate, followed by solvent evaporation to give a cast film, to which a methanol solution of the py-AuNPs (0.1 mg/mL) was spread and then air-dried. Finally, the film was washed with methanol several times and then air-dried to obtain the py-AuNPs/copolymer **1**/SWNT hybrid on the substrate. To prepare a sample for TEM measurements, a toluene solution of copolymer **1**/SWNTs was dropped onto a copper TEM grid, and then a methanol solution of py-AuNPs (0.1 mg/mL) was dropped, and then air-dried.

Preparation of a TFT Device. A doped silicon wafer with a 300-nm oxide was used as the substrate. Silicon dioxide layers were grown by a wet oxidization process. The source and drain electrodes were made

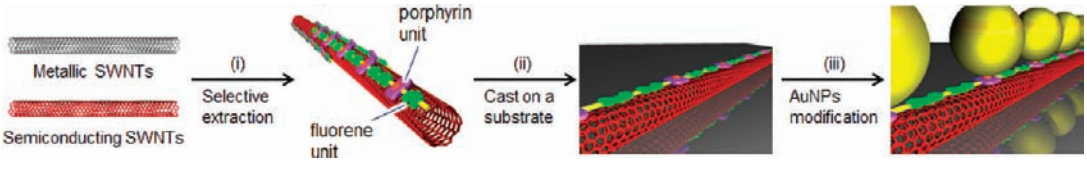

Figure 2. Design of a supramolecular hybrid of AuNPs, a copolymer of porphyrin and fluorene (shown in purple and green, respectively), and semiconducting SWNTs: (i) selective extraction of semiconducting SWNTs using a porphyrin−fluorene copolymer, (ii) cast film formation from the copolymer-wrapped semiconducting SWNTs solution on a substrate, and (iii) a supramolecular hybrid composed of AuNPs-coordinated porphyrin−fluorene copolymer-wrapped semiconducting SWNTs.

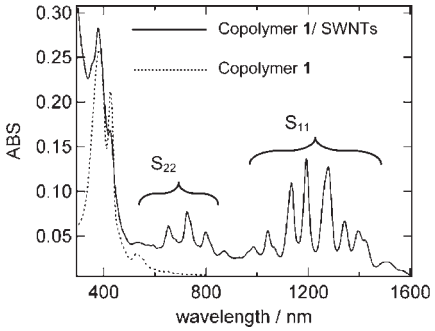

Figure 3. UV−vis−NIR absorption spectra of copolymer **1**/SWNTs (solid line) and copolymer **1** alone (dotted line) in toluene.

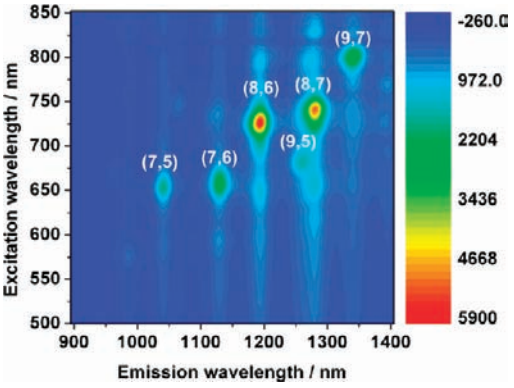

Figure 4. PL mapping image of the HiPco-SWNTs dissolved in copolymer **1** in toluene.

using a 50-nm Au coating patterned by a lift-off process. The length and width of the channel were 15 and 120 μm, respectively. A copolymer **1**/SWNTs solution was dropped onto the channel region between two Au electrodes and then air-dried. The dropping process was repeated until the devices could measure transfer properties, indicating the formation of a percolation path between the electrodes. The device was then annealed at 300 °C in a nitrogen environment for 2 h. The drain voltage was set at −20 V.

RESULTS AND DISCUSSION

The composition ratio of the porphyrin and fluorene units in the copolymer **1** was 1:10, and the weight-average molecular weight determined by GPC was M_w = 94 300, with M_w/M_n = 3.5. Copolymer **1** carries long alkyl chains and is soluble in many solvents, including toluene, chloroform, dichloromethane, and THF. It was found that in such solvents, except toluene, copolymer **1** individually solubilized both semiconducting and metallic SWNTs (data not shown) in a manner similar to other fluorene polymers and copolymers.

The vis−NIR absorption spectrum of copolymer **1**-solubilized SWNTs in toluene is shown in Figure 3, in which sharp S_{11} and S_{22} bands of the tubes are clearly observed in the ranges of 1000−1500 and 600−900 nm, respectively. In the range of 400−600 nm, we could not observe metallic SWNT band peaks, suggesting that copolymer **1**, like other many PFOs and their derivatives,[33,34] selectively dissolves the semiconducting SWNTs. Compared to that with copolymer **1** alone, the spectrum of the fluorene moiety on the copolymer **1**-solubilized SWNTs exhibited

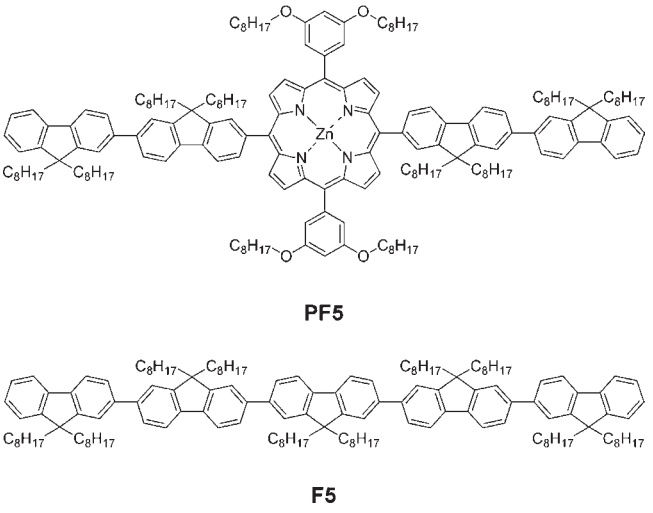

Figure 5. Chemical structures of **PF5** and **F5** for molecular mechanics simulation.

a 6-nm blue-shift of the peak around 390 nm, which is due to the interaction of the SWNTs and the fluorene moiety; i.e., it may arise from a decreased effective conjugation length of the copolymer on the copolymer **1**/ SWNT hybrid caused by the bulky porphyrin unit on the copolymer.[33,34]

PL spectroscopy[37] was used to determine the relative abundance of different species of semiconducting nanotubes in the copolymer **1**/SWNT solution. As shown in Figure 4, 2D-PL spots from individually dissolved SWNTs having chiral indices of (7,5), (7,6), (8,6), (8,7), (9,5), and (9,7) are observed; (8,6) and (8,7)SWNTs were especially enriched in the solution. The introduction of the porphyrin moiety to PFO slightly changed the extracted SWNT chirality; namely, although the 2D-PL mapping of the copolymer **1**-dissolved SWNTs resembled that of poly(9,9′-dioctylfluorene),[33,34] the (9,5) and (9,7)SWNTs were not recognized/extracted when PFO was used in place of copolymer **1**. We also used copolymer **2** in place of copolymer **1** and found that the chiral-selective SWNT solubilization behavior resembles that of copolymer **1** (see the Supporting Information, Figure S1), while we observed weak PL responses from (6,5), (8,4), (9,4), and (10,5)SWNTs in the copolymer **2**-solubilized solution that were not evident in the copolymer **1**-dissolved solution, indicating that high porphyrin unit in the copolymer reduces THE chiral selectivity of the SWNTs.

In an effort to understand the chiral-selective SWNT recognition/extraction, we carried out molecular mechanics simulations using the OPLS2005[38] force field to model the interactions between two types of pentamers, fluorene pentamer (**F5**) and porphyrin−fluorene oligomer (**PF5**) (Figure 5), and the (8,6) SWNTs. The binding energy of the wrapped SWNT is calculated by using eq 1,

$$E_{bind} = E_{comp} - (E_{poly} + E_{SWNT}) \quad (1)$$

where E_{comp}, E_{poly}, and E_{SWNT} represent the potential energies of the complex, polymer, and SWNTs, respectively.[39] The calculated results are shown in Table 1. The binding energy of the (8,6)SWNTs with **PF5** (−462.2 kcal/mol) was greater than that of the (8,6)SWNTs with **F5** (−430.5 kcal/mol), suggesting that **PF5** contributed to the wrapping of the SWNTs, which agrees with the fact that porphyrins are excellent SWNT

Table 1. Potential Energy (PE) and Energy Difference of the (8,6)SWNTs with the Porphyrin−Fluorene Tetramer (PF5) and Fluorene Pentamer (F5); All Energies in kcal/mol

	PE of oligomers, E_{poly}	PE of (8,6)SWNTs, E_{SWNT}	total PE, $E_{poly} + E_{SWNT}$	PE of complex, E_{comp}	binding energy $E_{bind} = E_{comp} - (E_{poly} + E_{SWNT})$
PF5	42.152	38 722.438	38 764.590	38 302.430	−462.160
F5	734.253	38 722.438	39 456.691	39 026.641	−430.05

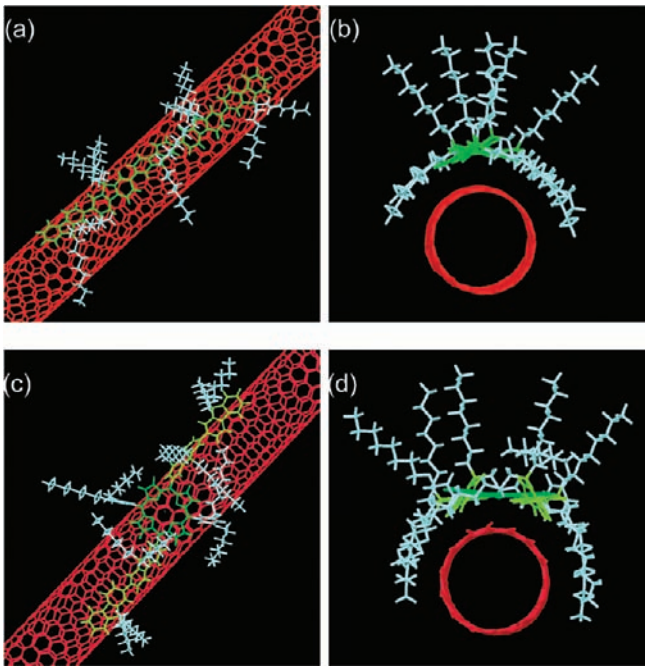

Figure 6. Model structures showing the top and side views of the (8,6) SWNTs with **PS** (a,b) and **PF5** (c,d).

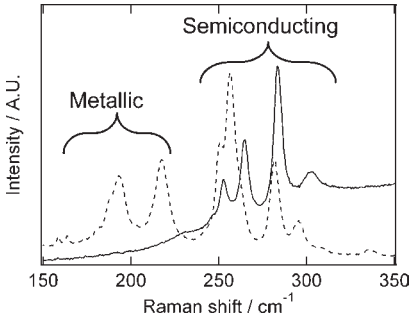

Figure 7. Raman spectra of the RBM frequencies of SWNTs solubilized by copolymer **1** (solid line) and the pristine SWNTs (broken line) excited at 633 nm.

solubilizers.[33,34] From the model, **F5** is aligned parallel (∼6°) to the long axes of the SWNTs (Figure 6a,b), while **PF5** is tilted at ∼12° relative to the long axes (Figure 6c,d) and the conformation of **PF5** is distorted. Molecular mechanics calculations of (9,5) and (9,7)SWNTs, which are virtually not dissolved by PFO, were carried out. In the case of (9,5)SWNTs with **PF5** and **F5**, the binding energies were calculated to be −465.8 and −427.2 kcal/mol, respectively, while in the case of (9,7) SWNTs with **PF5** and **F5**, the binding energies were −495.4 and −462.6 kcal/mol, respectively (for details, see the Supporting Information, Table S1), which explains the fact that copolymer **1** was able to solubilize (9,5) and (9,7)SWNTs. The calculated model structures of (9,5)SWNTs with **P5** and **F5** and of (9,7) SWNTs with **PF5** and **F5** (see the Supporting Information, Figure S2) resembled those of (8,6)SWNTs (Figure 6).

To confirm that the copolymer **1**-extracted SWNTs contain only semiconducting SWNTs, Raman spectra (633-nm excitation) of the extracted tubes were measured and compared to those of the pristine SWNTs. The radial breathing modes (RBMs) in the regions of 240−300 and 150−240 cm^{-1} in the SWNT Raman spectroscopy are attributed to the semiconducting and metallic SWNTs, respectively.[40] As shown in Figure 7, for the copolymer **1**-extracted SWNTs, we see clear peaks in the region of 240−300 cm^{-1} and no peak in the 150−240 cm^{-1} region, suggesting that the extracted SWNTs are the semiconducting SWNTs only, which agrees well with previous reports on PFOs and their derivatives.[33,34]

AFM was used to obtain direct images of the individually dissolved SWNTs. Figure 8 shows typical AFM images of copolymer **1**-dissolved SWNTs before (Figure 8a,e) and after (Figure 8b,f) the py-AuNP treatment on mica (Figure 8a,b) and on a silicon wafer (Figure 8e,f). From the line scans of the images, we obtained height profiles before (Figure 8c,g) and after (Figure 8d,h) the py-AuNP treatment on mica (Figure 8c,d) and on a silicon wafer (Figure 8g,h). The average diameters of the copolymer **1**/SWNTs on mica and the silicon wafer were estimated to be 4.2 ± 0.8 (Figure 8c) and 3.9 ± 0.5 nm (Figure 8g), respectively, which are larger than those of the SWNTs (diameters of (7,5), (7,6), (8,7), (8,7), (9,5), and (9,7) SWNTs are 0.829, 0.895, 0.966, 1.032, 0.976, and 1.103 nm, respectively).[41] The obtained diameters of the solubilized SWNTs suggest the SWNTs are wrapped by the copolymer **1**.

The height (12.1 ± 2.1 nm, Figure 8d) of the py-AuNP-treated sample on mica is greater than that of the copolymer **1**/SWNTs (4.2 ± 0.8 nm, Figure 8c). A similar result is obtained for the sample on the silicon wafer. This height difference was several times the diameter of the AuNP cores (2.7 ± 0.8 nm), suggesting that the py-AuNPs coordinated to the porphyrin units on the SWNTs.

As a control experiment, copolymer **1**/SWNTs on mica were treated with *t*-dode-AuNPs instead of py-AuNPs (see Supporting Information, Figure S3). The histogram shows that the average height of the structures was 4.5 ± 1.7 nm, which is almost identical to that of the copolymer **1**/SWNTs. It is evident that, without the pyridine moiety, the binding of the AuNPs with porphyrin units does not occur.

In Figure 9, we show the typical SEM and TEM images of the py-AuNPs-treated sample prepared on a silicon wafer and a copper grid. In both images, we can clearly see that the py-AuNPs are aligned along the SWNTs; the TEM image provides an especially clear image. The average diameter of the py-AuNPs in

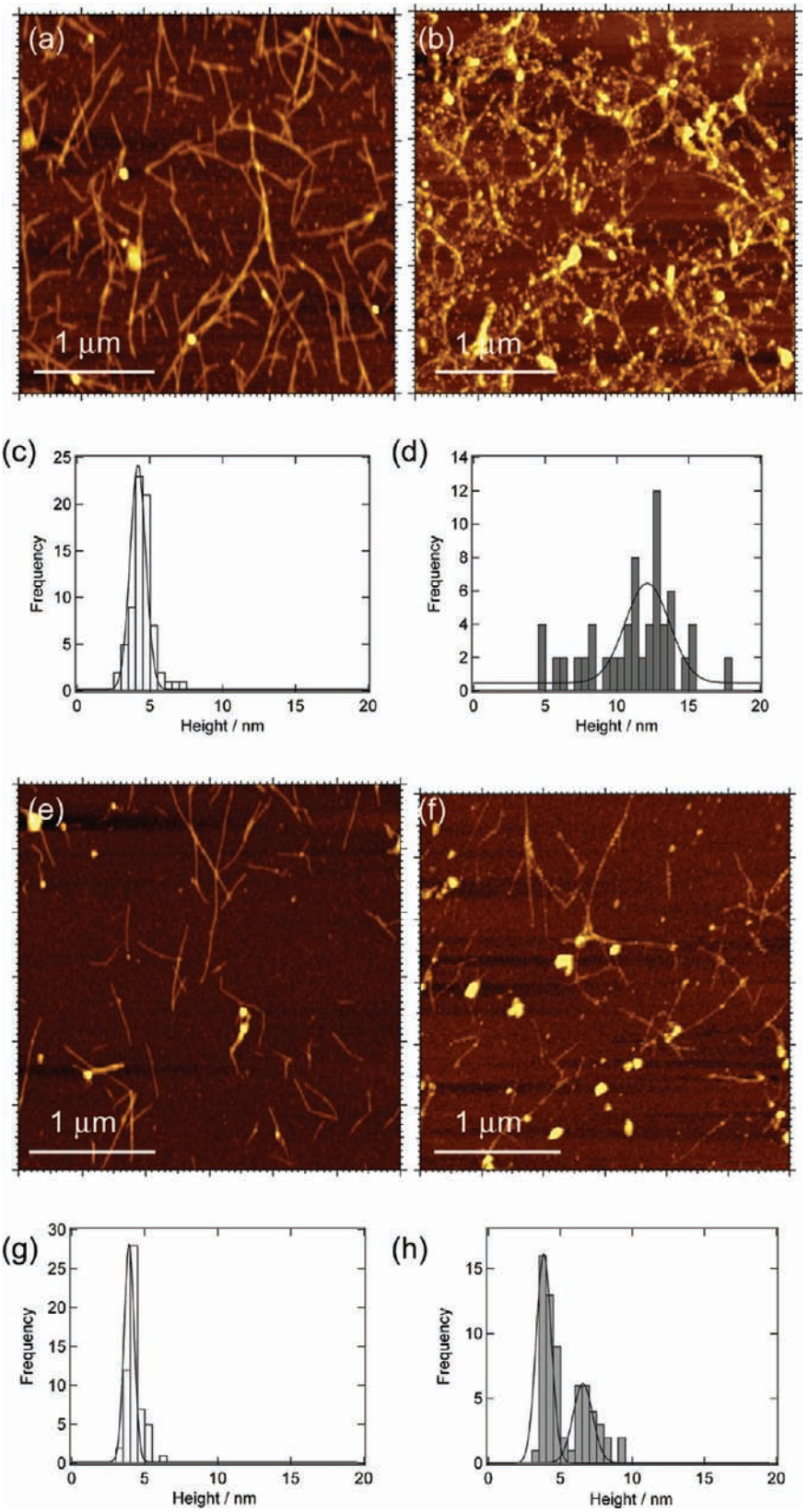

Figure 8. AFM images of (a) copolymer **1**/SWNTs and (b) py-AuNPs-coordinated copolymer **1**/SWNTs on mica surfaces, and height histograms of (c) copolymer **1**/SWNTs (4.2 ± 0.8 nm) and (d) py-AuNPs-coordinated copolymer **1**/SWNTs (12.1 ± 2.1 nm). AFM images of (e) copolymer **1**/SWNTs and (f) py-AuNPs-coordinated copolymer **1**/SWNTs on silicon wafers, and height histograms of (g) copolymer **1**/SWNTs (3.9 ± 0.5 nm) and (h) py-AuNPs-coordinated copolymer **1**/SWNTs (3.9 ± 0.7 and 6.6 ± 1.0 nm).

dx.doi.org/10.1021/ja2055885 |*J. Am. Chem. Soc.* 2011, 133, 14771–14777

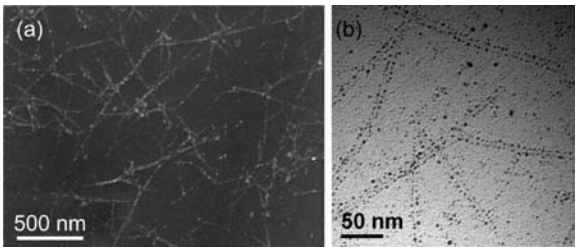

Figure 9. SEM (a) and TEM (b) images of the py-AuNPs-coordinated copolymer **1**-wrapped SWNTs on an undoped, naturally oxidized silicon substrate and a copper grid, respectively.

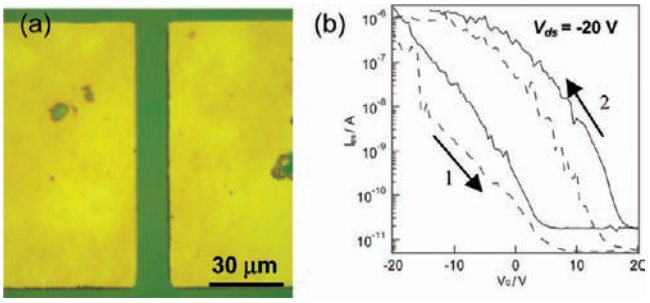

Figure 10. (a) Optical microscopy image of the TFT prepared from copolymer **1**/SWNTs and (b) typical transfer characteristics ($I_{SD}-V_G$) of the device before (broken line) and after (solid line) the py-AuNPs treatment. The numbers "1" and "2" indicate the scanning order of V_G.

the TEM was estimated to be ~5 nm, which is close to that of the AuNPs.

We carried out XPS measurements for samples of copolymer **1**/SWNTs after the py-AuNPs treatment and recognized peaks of the C (1s), N (1s), O (1s), S (2p), S (2s), Au (4d), and Au (4f) (see Supporting Information, Figure S4). The peaks of Au and S indicate the existence of the AuNPs and the pyridine ligand. This result also supports the formation of the supramolecular hybrid composed of py-AuNPs/copolymer **1**/semiconducting SWNTs.

We fabricated a TFT device using the copolymer **1**/SWNT hybrid before and after the py-AuNPs treatment and measured its transport properties. The channel length of the device was 15 μm (Figure 10a). A source−drain current (I_{SD}) vs gate-voltage (V_G) curve at room temperature was measured before and after the py-AuNPs modification, and the result is shown in Figure 10b. The fabricated TFT device showed a unipolar switching property with an evident p-type transport, and it showed and On/Off ratio of ~10^5, which is larger than or comparable to those of previously reported SWNTs TFT devices.[42−45] We then carried out the py-AuNP modification of the device and measured its transport property. Here, the On/Off ratio was ~10^5, and the device showed a unipolar switching property with a p-type transport, which is fundamentally similar to that of the device before the py-AuNP modification. However, it is revealed that, after the modification, the threshold voltage shifted in a positive direction, suggesting that the py-AuNPs acted as electron acceptors.[46] These results indicate that the py-AuNPs modification causes the copolymer **1**/SWNTs to change electrical properties. Such device performance might be useful for designing new types of sensor devices.[47−49]

CONCLUSIONS

We synthesized a new copolymer consisting of porphyrin and fluorene backbones and extracted semiconducting (8,6)- and (8,7)-enriched SWNTs without metallic tubes, which were connected to AuNPs via coordination bonding between the pyridine-terminated AuNPs and the zinc metal of the porphyrin on the copolymer. The obtained supramolecular hybrid contains many functional groups, including porphyrin, fluorene, metal nanoparticles, and semiconducting SWNTs, and is of interest over a wide area of nanomaterials science and technology. We have also demonstrated that a TFT device using the hybrid shows p-type transport, with an On/Off ratio of ~10^5, and changes transport properties after the AuNPs modification. Such a unique property would be useful in designing future electronic devices based on carbon nanotubes. Fine-tuning of the TFT performance by attaching different metal nanoparticles, including semiconducting nanoparticles, is currently underway in our laboratory.

ASSOCIATED CONTENT

Supporting Information. MD calculation for (9,5) and (9,7)SWNTs, PL using copolymer **2**, additional AFM images of SWNTs after treatment with *t*-dode-AuNPs, and XPS data. This material is available free of charge via the Internet at http://pubs.acs.org.

AUTHOR INFORMATION

Corresponding Author
nakashima-tcm@mail.cstm.kyushu-u.ac.jp

ACKNOWLEDGMENT

This work was supported by a Grant-in-Aid for Scientific Research (B) (No. 17205014 for N.N.), Nanotechnology Network Project (Kyushu-area Nanotechnology Network), and Global COE Program (Science for Future Molecular Systems) from the Ministry of Education, Culture, Sports, Science and Technology, Japan. We thank Dr. Fumiyuki Toshimitsu of Kyushu University for molecular mechanics calculation and Prof. A. Robertson and Dr. M. R. Berber for helpful discussions. We also thank Ms. Natsuko Ide for technical assistance.

REFERENCES

(1) D'Souza, F., Kadish, K. M., Eds. *Handbook of Carbon Nano Materials*; World Scientific: Hackensack, NJ, 2011.
(2) Guldi, D. M., Martin, N., Eds. *Carbon Nanotubes and Related Structures*; Wiley-VCH: Weinheim, 2010.
(3) Akasaka, T., Wudl, F., Nagase, S., Eds. *Chemistry of Nanocarbons*; John Wiley & Sons: Chichester, 2010.
(4) Basiuk, V. A., Basiuk, E. V., Eds. *Chemistry of Carbon Nanotubes*; American Scientific Publishers: Valencia, CA, 2008.
(5) O'Connell, M. J.; Bachilo, S. M.; Huffman, C. B.; Moore, V. C.; Strano, M. S.; Haroz, E. H.; Rialon, K. L.; Boul, P. J.; Noon, W. H.; Kittrell, C.; Ma, J.; Hauge, R. H.; Weisman, R. B.; Smalley, R. E. *Science* **2002**, *297*, 593–596.
(6) Fukushima, T.; Kosaka, A.; Ishimura, Y.; Yamamoto, T.; Takigawa, T.; Ishii, N.; Aida, T. *Science* **2003**, *300*, 2072–2074.
(7) Arnold, M. S.; Stupp, S. I.; Hersam, M. C. *Nano Lett.* **2005**, *5*, 713–718.

(8) Teo, K. B. K.; Minoux, E.; Hudanski, L.; Peauger, F.; Schnell, J.-P.; Gangloff, L.; Legagneux, P.; Dieumegard, D.; Amaratunga, G. A. J.; Milne, W. I. *Nature* **2005**, *437*, 968.
(9) Futaba, D. N.; Hata, K.; Yamada, T.; Hiraoka, T.; Hayamizu, Y.; Kakudate, Y.; Tanaike, O.; Hatori, H.; Yumura, M.; Iijima, S. *Nat. Mater.* **2006**, *5*, 987–994.
(10) Paolucci, D.; Franco, M. M.; Iurlo, M.; Marcaccio, M.; Prato, M.; Zerbetto, F.; Pénicaud, A.; Paolucci, F. *J. Am. Chem. Soc.* **2008**, *130* 7393–7399.
(11) Tanaka, Y.; Hirana, Y.; Niidome, Y.; Kato, K.; Saito, S.; Nakashima, N. *Angew. Chem., Int. Ed.* **2009**, *48*, 7655–7659.
(12) Hirana, Y.; Tanaka, Y.; Niidome, Y.; Nakashima, N. *J. Am. Chem. Soc.* **2010**, *132*, 13072–13077.
(13) Shin, H.-J.; Choi, W. M.; Choi, D.; Han, G. H.; Yoon, S.-M.; Park., H.-K.; Kim, S.-W.; Jin, Y. W.; Lee, S. Y.; Kim, J. M.; Choi, J.-Y.; Lee, Y. H. *J. Am. Chem. Soc.* **2010**, *132*, 15603–15609.
(14) Tu, X.; Manohar, S.; Jagota, A.; Zheng, M. *Nature* **2009**, *460*, 250–253.
(15) Matsumoto, K.; Fujigaya, T.; Yanagi, H.; Nakashima, N. *Adv. Funct. Mater.* **2011**, *21*, 1089–1094.
(16) Lee, C. Y.; Choi, W.; Han, J.-H.; Strano, M. S. *Science* **2010**, *329*, 1320–1324.
(17) Singh, R.; Premkumar, T.; Shin, J. Y.; Geckeler, K. E. *Chem.—Eur. J.* **2010**, *16*, 1728–1743.
(18) Peng, X. H.; Chen, J. Y.; Misewich, J. A.; Wong, S. S. *Chem. Soc. Rev.* **2009**, *38*, 1076–1098.
(19) Bottini, M.; Dawson, M. I.; Mustelin, T. In *Chemistry of Carbon Nanotubes*; Basiuk, V. A., Basiuk, E. V., Eds.; American Scientific Publishers: Valencia, CA, 2008; pp 25−34.
(20) Jiang, K.; Eitan, A.; Schadler, L. S.; Ajayan, P. M.; Siegel, R. W.; Grobert, N.; Mayne, M.; Reyes-Reyes, M.; Terrones, H.; Terrones, M. *Nano Lett.* **2003**, *3*, 275–277.
(21) Kim, B.; Sigmund, W. M. *Langmuir* **2004**, *20*, 8239–8242.
(22) Rahman, G. M. A.; Guldi, D. M.; Zambon, E.; Pasquato, L.; Tagmatarchis, N.; Prato, M. *Small* **2005**, *1*, 527–530.
(23) Sainsbury, T.; Fitzmaurice, D. *Chem. Mater.* **2004**, *16*, 2174–2179.
(24) Biju, V.; Itoh, T.; Makita, Y.; Ishikawa, M. J. *Photochem. Photobiol. A* **2006**, *183*, 315–321.
(25) Ellis, A. V.; Vjayamohanan, K.; Goswaimi, R.; Chakrapani, N.; Ramanathan, L. S.; Ajayan, P. M.; Ramanath, G. *Nano Lett.* **2003**, *3* 279–282.
(26) Ou, Y.-Y.; Huang, M. H. *J. Phys. Chem. B* **2006**, *110*, 2031–2036.
(27) Han, X. G.; Li, Y. L.; Deng, Z. X. *Adv. Mater.* **2007**, *19* 1518–1522.
(28) Wang, D.; Li, Z. C.; Chen, L. W. *J. Am. Chem. Soc.* **2006**, *128*, 15078–15079.
(29) Raghuveer, M. S.; Agrawal, S.; Bishop, N.; Ramanath, G. *Chem. Mater.* **2006**, *18*, 1390–1393.
(30) Choi, H. C.; Shim, M.; Bangsaruntip, S.; Dai, H. *J. Am. Chem. Soc.* **2002**, *124*, 9058–9059.
(31) Li, X.; Qin, Y.; Picraux, S. T.; Guo, Z.-X. *J. Mater. Chem.* **2011**, *21*, 7527–7547.
(32) Ozawa, H.; Fujigaya, T.; Niidome, Y.; Hotta, N.; Fujiki, M.; Nakashima, N. *J. Am. Chem. Soc.* **2011**, *133*, 2651–2657 and references cited therein.
(33) Nish, A.; Hwang, J. Y.; Doig, J.; Nicholas, R. J. *Nature Nanotechnol.* **2007**, *2*, 640–646.
(34) Chen, F. M.; Wang, B.; Chen, Y.; Li, L. J. *Nano Lett.* **2007**, *7* 3013–3017.
(35) Zhang, X. C.; Zhang, Y.; Wang, C. Y.; Lai, G. Q.; Zhang, L.; Shen, Y. J. *Polym. Bull.* **2009**, *63*, 815–827.
(36) Ozawa, H.; Kawao, M.; Tanaka, H.; Ogawa, T. *Langmuir* **2007**, *23*, 6365–6371.
(37) Bachilo, S. M.; Strano, M. S.; Kittrell, C.; Hauge, R. H.; Smalley, R. E.; Weisman, R. B. *Science* **2002**, *298*, 2361–2366.
(38) Fariborz, M.; Nigel, G. J. R.; Wayne, C. G.; Rob, L.; Mark, L.; Craig, C.; George, C.; Thomas, H.; Still, W. C. *J. Comput. Chem.* **1990**, *11*, 440–467.
(39) Yan, L. Y.; Li, W. F.; Fan, X. F.; Wei, L.; Chen, Y.; Kuo, J. L.; Li, L. J.; Kwak, S. K.; Mu, Y. G.; Chan-Park, M. B. *Small* **2010**, *6*, 110–118.
(40) Kataura, H.; Kumazawa, Y.; Maniwa, Y.; Umezu, I.; Suzuki, S.; Ohtsuka, Y.; Achiba, Y. *Synth. Met.* **1999**, *103*, 2555–2558.
(41) Weisman, R. B.; Bachilo, S. M. *Nano Lett.* **2003**, *3*, 1235–1238.
(42) Izard, N.; Kazaoui, S.; Hata, K.; Okazaki, T.; Saito, T.; Iijima, S.; Minami, N. *Appl. Phys. Lett.* **2008**, *92*, 243112.
(43) Zhang, L.; Tu, X. M.; Welsher, K.; Wang, X. R.; Zheng, M.; Dai, H. J. *J. Am. Chem. Soc.* **2009**, *131*, 2454–2455.
(44) Asada, Y.; Miyata, Y.; Shiozawa, K.; Ohno, Y.; Kitaura, R.; Mizutani, T.; Shinohara, H. *J. Phys. Chem. C* **2011**, *115*, 270–273.
(45) Asada, Y.; Miyata, Y.; Ohno, Y.; Kitaura, R.; Sugai, T.; Mizutani, T.; Shinohara, H. *Adv. Mater.* **2010**, *22*, 2698–2701.
(46) Jeong, G. H. *Trans. Nonferrous Met. Soc. China* **2009**, *19*, 1009–1012.
(47) Kim, S. N.; Rusling, J. F.; Papadimitrakopoulos, F. *Adv. Mater.* **2007**, *19*, 3214–3228.
(48) Allen, B. L.; Kichambare, P. D.; Star, A. *Adv. Mater.* **2007**, *19*, 1439–1451.
(49) Sinha, N.; Ma, J. Z.; Yeow, J. T. W. *J. Nanosci. Nanotechnol.* **2006**, *6*, 573–590.